On the existing and new potential methods for Partial Discharge source monitoring in electrical power grids

Denis Stanescu[1,2][0000-0001-5138-9843], Angela Digulescu[1,2][0000-0002-1561-3286], Cornel Ioana[1][0000-0001-6581-3000] and Alexandru Serbanescu[2][0000-0003-0044-3971]

[1] University of Grenoble Alpes, GIPSA-lab, France
[2] Military Technical Academy "Ferdinand I", Romania
denis.stanescu@gipsa-lab.grenoble-inp.fr

Abstract. Power transmission and distribution networks currently face an intensive use and climate change challenges. In such networks, the occurrence of defaults (caused by the cable ageing process, the structure and network capacity, voltage levels, and related environmental conditions) is inevitable. The difficulties of predictive maintenance of power grids are related to the large spread of electrical infrastructures and the definition of early warning indicators. Such indicators are the partial discharge activities which are very informative about the rising insulation problems of electrical materials. The monitoring of such phenomena is nowadays an important field in the power transmission and distribution systems. The purpose of this paper is to study different techniques for the detection of transient signals in the context of monitoring partial discharges in electrical networks. Among the various techniques developed and used for the detection of partial discharges, we will focus here on four classes of methods; two of them are encountered in existing products, whereas two new techniques are based on recent concepts: compressive sensing and phase-diagram based analysis. The comparative study concerns the evaluation of the probability of detection versus false alarm ratio of real signals measured on a reduced scale experimental facility. Thanks to this experimental facility typical for real life configurations, we are able to add to the partial discharge signals perturbations such as load signals, reflections but also the effect of propagation effects in a real electrical cable which allow us to highlight the performances of each method.

Keywords: Partial Discharge, transient analysis, network monitoring, compressive sensing, phase-diagram analysis.

1 Introduction

In the study of electrical networks, when a cable starts to be damaged, its dielectric properties are affected and they may conduct to the power outage if the rising faults are not detected. The dielectric problems in cables generate partial discharges that are transient signals, subject to the effects of propagation, deformation, reflection, etc. Moreover, there is the possibility that different external accessories are connected to

the network. These loads generate a unique signal that does not produce reflected or distorted additional versions of its own, but since it is usually much closer to the sensor than the partial discharges sources, their magnitude is much higher than the one of the partial discharges. This complicates the process of network monitoring, in order to accurately detect the partial discharge source leading to the appearance of false alarms or a large number of detected signals [1]. In this context, the aim of this paper is to study comparatively the state-of-the art detection techniques as well as the new techniques, recently proposed. Section 2 presents the methods used in this paper for the detection of partial discharges, four classes of methods being considered. Section 3 contains the results obtained by applying each method and a comparison of the effects of their use and section 4 presents the conclusions and perspectives of this work.

2 Theoretical aspects

2.1 Spectrogram

The Short Time Fourier Transform (STFT), the oldest and also the most used time-frequency analysis method, was introduced to be able to measure the frequency variations of a signal by calculating the Fourier transform of a window of the analyzed signal, the window moving along the time axis according to eq. 1, where $s(t)$ is the signal to be analyzed, $g(t)$ is the limited window signal centered in *u*.

$$S(u, f) = \int_{-\infty}^{\infty} s(t) g^*(t-u) e^{-j2\pi ft} dt \tag{1}$$

Using this transform, the energy density of the signal is defined, namely the spectrogram, as in the eq. 2, which measures the energy of the signal in a time-frequency cell.

$$P_S(u, f) = \left|S(u, f)\right|^2 = \left|\int_{-\infty}^{\infty} s(t) g^*(t-u) e^{-j2\pi t} dt\right|^2 \tag{2}$$

Time-frequency resolution is an important parameter of this method and is influenced by the analysis window, whose length should be small enough so that the window signal is stationary over the considered interval and large enough for the Fourier transform to provide reasonable frequency information. The STFT has been naturally used for the detection of partial discharge activities as shown in [2] and [3].

From the STFT representation the Detection Curve (DC) is computed as the marginal in time with the following equation:

$$DC(u) = \left\{ \sum_f P_s(u, f) \geq \alpha \right\} \tag{3}$$

The detection of PD activity corresponds to the time moment for which the frequency signature of the partial discharge is higher than an imposed threshold α , this being the basis of which the detection curves are built.

2.2 Wavelet Transform

The Wavelet transform is a linear transformation used to decompose a signal $s(t)$ into an orthonormal basis consisting of a family of functions $\psi(t)$ called wavelets, where m is the scaling factor, n is the time shift factor and ψ_0 the generator wavelet [4].

$$\psi(t) = \frac{1}{\sqrt{m}} \psi_0 \left(\frac{t-n}{m} \right) \tag{4}$$

The central idea is based on the proposal of an orthonormal base elaborated from a generating wavelet, of average zero and its dilated and delayed variants in order to assure the decomposition of the analyzed signal using eq. 5:

$$W_\psi(n,m) = \int_{-\infty}^{\infty} s(t) \psi^*(t) dt \tag{5}$$

As a result of this design, a two-dimensional function is obtained, namely the scalogram, which reproduces the signal energy distribution for the scale m and the position in time n [4]. To compute the detection curve, eq. 6 is used:

$$DC(n) = \left\{ \sum_m W_\psi(n,m) \geq \alpha \right\} \tag{6}$$

which captures the appearance of the signal of interest for which its energy distribution exceeds a certain threshold α .

2.3 Compressive sensing

The background of compressive sensing, which is a recent topic in nowadays signal processing research field, is based on the possibility of obtaining a signal from its incomplete version, affected by problems such as the loss of a number of samples from it.

Starting from a signal $s[n]$ that exhibits sparsity in an $N \times 1$ orthonormal basis $\psi = \{\psi_1, \psi_2, ..., \psi_N\}$, it is possible to represent it using its sparse transform domain $N \times 1$ vector $x = \{x_1, x_2, ..., x_N\}$ using the matrix notation from eq.7 [5].

$$\mathbf{s} = \mathbf{\Psi} \cdot \mathbf{x} \tag{7}$$

Using the compressive sensing approach, it is possible to reduce the sampling rate of the sparse signal, with the help of a reduced signal $y[m]$ of length *M*, where $M < N$. To model the reduced signal, the matrix notation from eq.8 is used:

$$\mathbf{y}=\mathbf{A}\cdot\mathbf{x} \tag{8}$$

where $\mathbf{A}$ is the measurement matrix through which projections of the signal onto vectors of the matrix were achieved. The Eq. 9 gives us the sparse transform domain representation unfolded:

$$\begin{bmatrix} y[0] \\ y[1] \\ \vdots \\ y[M-1] \end{bmatrix} = \begin{bmatrix} \alpha_0[0] & \alpha_1[0] & \cdots & \alpha_{N-1}[0] \\ \alpha_0[1] & \alpha_1[1] & \cdots & \alpha_{N-1}[1] \\ \vdots & \vdots & \ddots & \vdots \\ \alpha_0[M-1] & \alpha_1[M-1] & \cdots & \alpha_{N-1}[M-1] \end{bmatrix} \cdot \begin{bmatrix} x[0] \\ x[1] \\ \vdots \\ x[N-1] \end{bmatrix} \tag{9}$$

where $\alpha_k[m]$ are the coefficients of the measurement matrix . If the number of the nonzero coefficients of the vector $\mathbf{x}$, denoted by K, is much smaller than the total number of samples *N*, the vector $\mathbf{x}$ is considered to be sparse [6].

$$x[k]=0,\ k\neq\{k_1,k_2,...,k_K\},\ K<N \tag{10}$$

The signal reconstruction problem is based on the reconstruction of vector $\mathbf{x}$ from the eq. 8. For this, assuming the known position of the zero coefficients, if we eliminate the columns corresponding to them from the measurement matrix $\mathbf{A}$, the system from eq. 8 becomes:

$$\mathbf{y}=\mathbf{A}_K\cdot\mathbf{x}_K \tag{11}$$

with $\mathbf{A}_K$ a $M\times K$ matrix specific to the nonzero coefficients. From the minimization of the difference between the reduced signal and the reconstructed values $\mathbf{x}_K$:

$$e^2=\|y-A_K x_K\|^2=(y-A_K x_K)^H(y-A_K x_K) \tag{12}$$

where *H* denotes the Hermitian transpose conjugate, we obtain the solution of the system, which means the reconstructed signal according to eq.13.

$$x_K=\left(A_K^H A_K\right)^{-1}A_K^H y \tag{13}$$

In this paper, we assumed that the signal is sparse in the STFT. More details on this method can be found in [6] and [7]. For the detection part, the considerations discussed in section 2.1 were used:

$$DC(u)=\left\{\sum_{f} P_{\mathbf{x}_K}(u,f)\geq\alpha\right\} \tag{14}$$

in which $P_{\mathbf{x}_K}(u,f)$ represents the spectrogram of the signal $\mathbf{x}_K$ and α is the value for the specific threshold.

2.4 Phase-diagram-based analysis

This method is used for non-linear data analysis, in order to characterize a dynamical system where certain nonlinear properties can indicate changes in system behavior. Starting from a time series, like the one in eq. 15, the strategy for the phase space trajectory design is given by moving from the initial values of the time series to a vector that defines the new representation space (eq. 16).

$$s=\{s[1],s[2],...,s[N]\} \tag{15}$$

$$\overrightarrow{v_{[i]}}=\sum_{k=1}^{m} s\left[i+(k-1)d\right]\cdot\overrightarrow{e_k} \tag{16}$$

where $\overrightarrow{v_{[i]}}$ are the vectors of the phase space, m is the embedding dimension of the phase space, d is the delay chosen between the samples, $\overrightarrow{e_k}$ is the unit vector of the axis. In determining the parameters, the mutual information method is usually used to establish the delay and the false nearest neighbor method for the encapsulation size [8].

In order to highlight the algorithm for estimating the instantaneous frequency, used in the detection process, we will present the algorithm starting from a sinusoidal signal expressed by eq. 17.

$$s[n]=\sin(2\pi f_0\frac{n}{f_s}),\ n=\left\{0,1,...,\frac{2f_s}{f_o}\right\} \tag{17}$$

where $f_0=3$ and $f_s=30$. The signal and the phase space representation can be seen in Fig. 1.

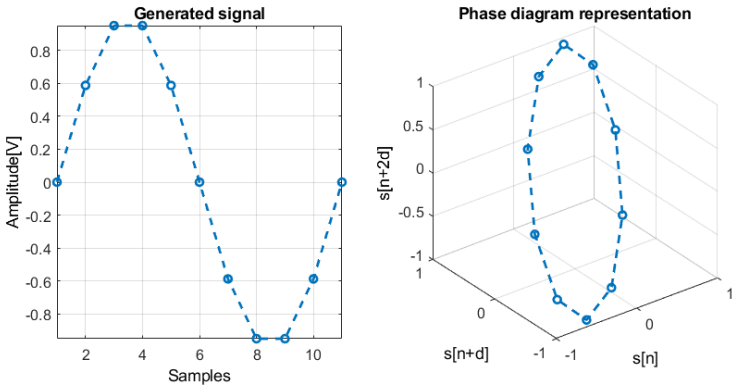

Fig. 1. The generated signal from eq. 17 (left); the phase diagram trajectory for the signal from eq. 17 (right)

After the new trajectory of the signal is computed, it is necessary to quantify the number of recurrent points and for that for each pair of points, the angle between two position vectors is calculated using eq. 18.

$$\alpha_i = \arccos\left(\frac{\overrightarrow{v_{[i]}} \cdot \overrightarrow{v_{[i+1]}}}{\left|\overrightarrow{v_{[i]}}\right| \cdot \left|\overrightarrow{v_{[i+1]}}\right|}\right) \tag{18}$$

The angular distance must meet a certain condition, since for two points to be recurrent it is necessary the existence of a rotation of the position vectors in the phase space.

$$N_k \ \textit{is given by} \sum_{j=i}^{i+N_k-1} \alpha_j = \pi \tag{19}$$

Determining the number of points, we can estimate the fundamental frequency of the signal, using eq. 20, where N_k represents the number of recurring points for a semi-rotation and f_s is the sampling frequency of the analyzed signal.

$$f_k = \frac{f_s}{2N_k} \tag{20}$$

Thus the instantaneous frequency law can be estimated:

$$IFL(k) = \frac{f_s}{2N_k}, \text{ where } N_k \mid \sum_{j=i}^{i+N_k-1} \alpha_j = \pi \tag{21}$$

From here, we can reach at a general form of instantaneous frequency law estimation using the phase diagram for a random signal $s_{IFL} = \sin(\phi(t))$ with the phase of the signal $\phi(t)$.

$$IFL = \frac{1}{2\pi}\frac{\partial\phi(t)}{\partial t} \tag{22}$$

Eq. 23 was used to construct the detection curve, α representing also in this case a value of an imposed detection threshold:

$$DC = \left\{1 - \frac{IFL}{\max(IFL)} \geq \alpha\right\} \tag{23}$$

More details on the use and application of the algorithm can be found in [8].

3 Experimental configuration and results

To support the study of detection an experimental workbench was developed, the electrical network created can be seen in Fig 2. It consists in 914 meters length grid, three reduced scale substations (P1-P3), two loads (motor and heating circuit), one partial discharge source and three local sending units.

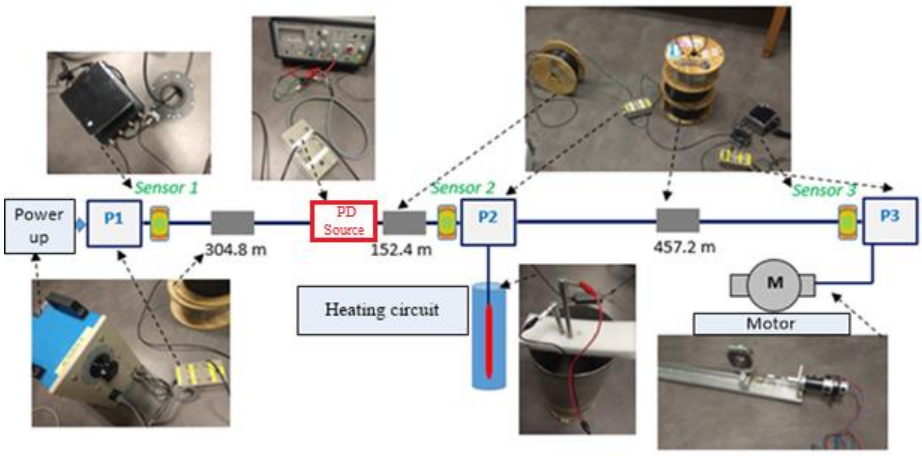

Fig. 2. Experimental facility

In the first phase, the impact of the two accessories on the network is studied, performing an analysis of the signal transmitted in the network in the presence of partial discharges, Fig. 3 showing the two situations. The signals were acquired with a duration of *6 ms* and a sampling frequency of *200MHz*.

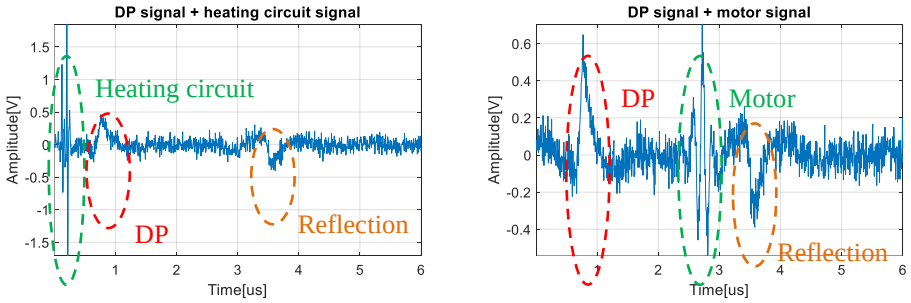

Fig. 3. The signal transmitted in the network in the presence of the DP signal and: heating circuit (left), motor (right)

Using the STFT-based approach, the detection curves observed in Fig. 4 are obtained. To determine the spectrogram of the signal, a Hamming window of 64 samples size was used, after which the sum of the columns is applied so that the detection curve is obtained. As it can be seen, the signal introduced by the heating circuit has a higher amplitude than the partial discharge, this leading to problems related to its detection. The low level of the DP signal and its reflection make it impossible to detect the fault by choosing an inappropriate threshold, a prior view being necessary in order to make a decision. Obtaining the detection curve in the case of the motor in the circuit co-existence, its separation from the useful signal is impossible, the magnitude level being the same for the two signals.

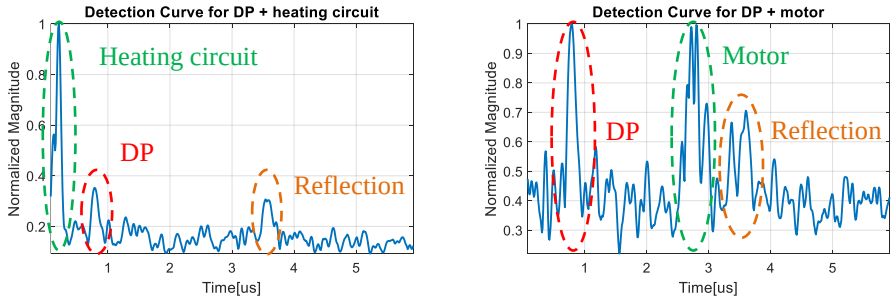

Fig. 4. The detection curves using spectrogram approach for the two situations

The use of the Wavelet transform method involves determining the optimal scale required for the detection process. As seen in Fig. 5, the existence of a high number of time-scale representations complicates the detection process. The type of wavelet used in this paper was given by the Daubechies family, as it corresponded best to the existing situation.

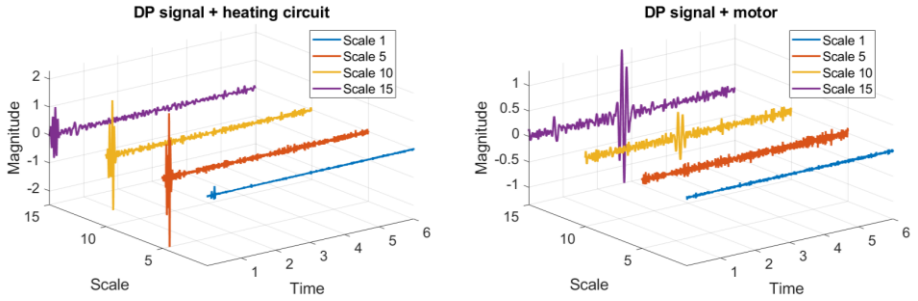

Fig. 5. Representation of the different time-scale components obtained by applying the wavelet transform for the 2 situations

Although, by determining the detection curves shown in Fig. 6, the DP is highlighted, the existence of local maxima can lead to false detections. Not knowing the shape and size of the analysis signal, there are problems given the choice of the wavelet, and in this case a visual evaluation is needed. In this case, there is also the problem related to setting the detection threshold.

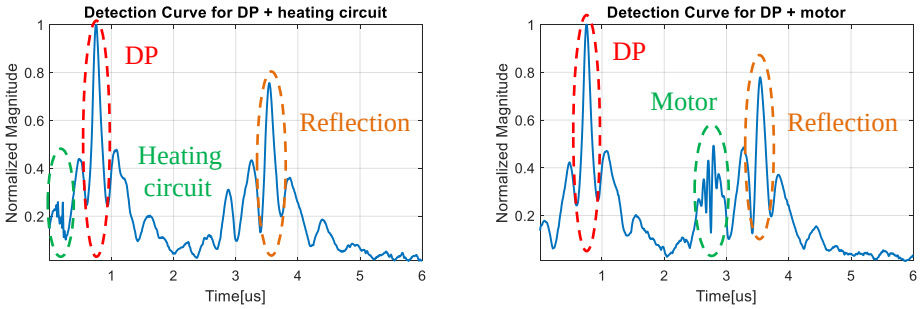

Fig. 6. The detection curves using wavelet approach for the two situations

The compressive sensing approach is used in combination with the spectrogram to see if there are any improvements to the method being respected the same considerations as in the case of developing the initial method. According to Fig. 7, the process of detecting transients is easier in this case. The detection curve shows a lower number of possible false alarms resulting from choosing an inappropriate threshold, but the constraints related to the use of the spectrogram remain valid.

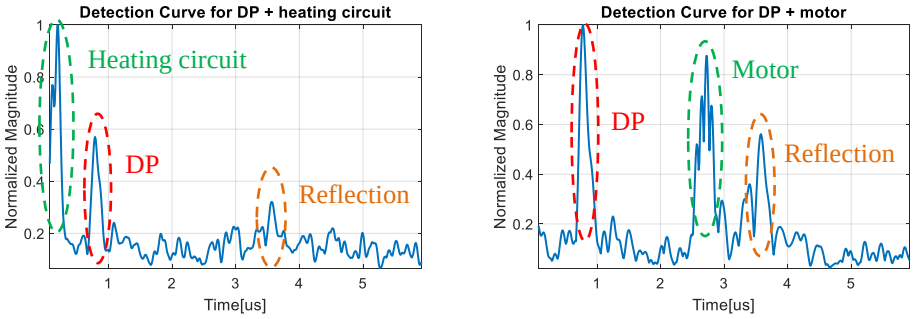

Fig. 7. The detection curves using the spectrogram approach after applying the compressive sensing algorithm for the two cases

By estimating the instantaneous frequency law of the signal using the phase diagram, the time moments of the appearance of the different transients can be highlighted, being eliminated the necessity of the existence of the detection threshold as can be seen in Fig. 8. From the perspective of the parameters of interest, following the calculations, the value $d = 4$ is obtained for the time delay and for the encapsulation dimension $m = 3$. Depending on the frequency content, a decision can be made regarding the nature of the transient.

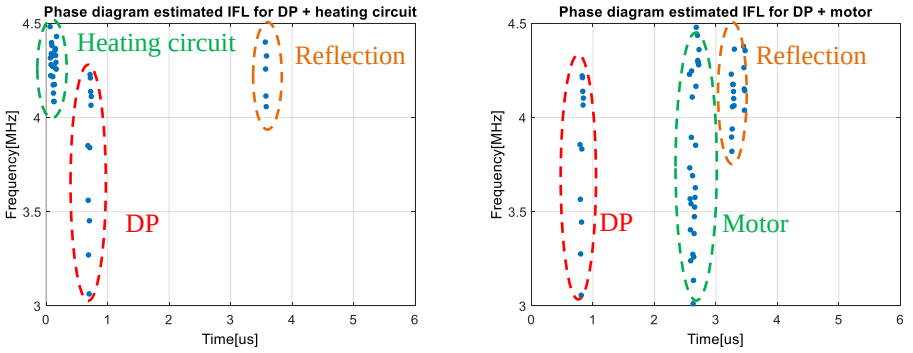

Fig. 8. The instantaneous frequency law estimation using the phase diagram approach for the two situations

In order to quantify the information revealed so far, the ROC curves are computed which help us to observe the performances of each analysis method, as shown in Fig. 9.

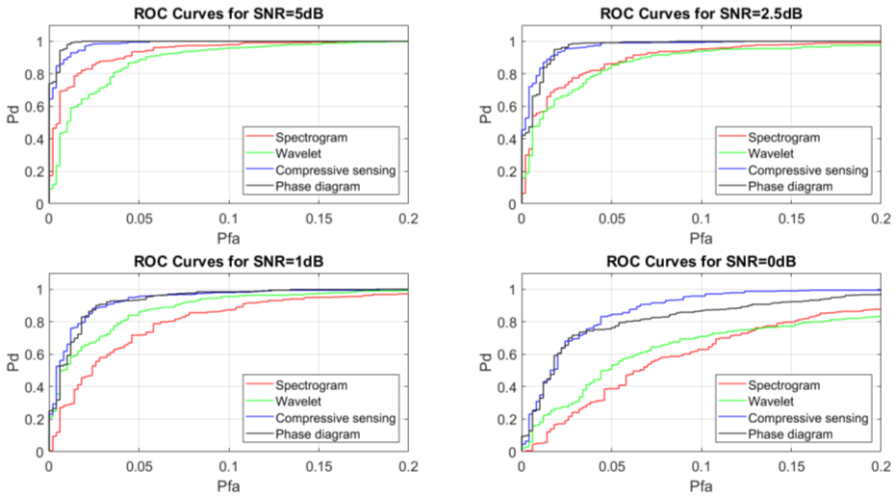

Fig. 9. ROC Curves for the four approaches

The two proposed methods, based on newer concepts, bring us a higher performance than the two classic methods. These can make a beneficial contribution to the usual methods of analysis.

4 Conclusions

In this paper we make a comparison between different methods used to detect partial discharges in an electrical system, focusing on two classic methods, widely used and two more recent methods that can be used for these types of applications.

The major advantage of the two new methods is that they do not depend in their analysis on the shape of the signal, unlike the Wavelet transform. We also show that the method based on compressive sensing can be used in combination with the spectrogram so that the level of accuracy of the result is higher.

The estimation of instantaneous frequency laws is successfully done using the phase diagram analysis by associating time-frequency points according to the criteria defined by this method. This highlights the coexistence of signals even in noise conditions and is robust while the noise level is minimized. In future works, the use of entropy can be a very interesting way to quantify the information represented in time-frequency domain [9].

Acknowledgment

This work has been realized in the CLASS_T project framework, supported by the Auvergne-Rhone-Alpes Region funding - Pack Ambition Recherche program.

References

1. Stone, G.C.: Partial discharge diagnostics and electrical equipment insulation condition assessment. IEEE Trans. Dielect. Electr. Insul. 12, 891–903 (2005).
2. Gottin, B., Ioana, C., Chanussot, J., D'Urso, G., Espilit, T.: Detection and Localization of Transient Sources: Comparative Study of Complex-Lag Distribution Concept Versus Wavelets and Spectrogram-Based Methods. EURASIP J. Adv. Sig. Proc. 2009, (2009).
3. Van Der Wielen, P., Steennis, F.: First field experience of on-line partial discharge monitoring of MV cable systems with location. In: IET Conference Publications. pp. 70–70. IET, Prague, Czech Republic (2009).
4. Mallat, S.: A Wavelet Tour of Signal Processing. Academic Press, San Diego (2009).
5. Stanković, S., Ioana, C., Li, X., Papic, V.: Algorithms for Compressive Sensing Signal Reconstruction with Applications. Mathematical Problems in Engineering. 2016, 1–3 (2016).
6. Stanković, L., Sejdić, E., Stanković, S., Daković, M., Orović, I.: A Tutorial on Sparse Signal Reconstruction and Its Applications in Signal Processing. Circuits Syst Signal Process. 38, 1206–1263 (2019).
7. Stanković, I., Ioana, C., Daković, M.: On the reconstruction of nonsparse time-frequency signals with sparsity constraint from a reduced set of samples. Signal Processing. 142, 480–484 (2018).
8. Digulescu, A., Ioana, C., Serbanescu, A.: Phase Diagram-Based Sensing with Adaptive Waveform Design and Recurrent States Quantification for the Instantaneous Frequency Law Tracking. Sensors. 19, 2434 (2019).
9. Saulig, N., Milanović, Ž., Ioana, C.: A local entropy-based algorithm for information content extraction from time–frequency distributions of noisy signals. Digital Signal Processing. 70, 155–165 (2017).